



Article

Electrospun Nanofibrous Mesh Based on PVA, Chitosan, and Usnic Acid for Applications in Wound Healing

Alexandra Elena Stoica (Oprea)¹, Delia Albuleț¹, Alexandra Cătălina Bîrcă¹, Florin Iordache^{2,3} , Anton Ficăi¹ , Alexandru Mihai Grumezescu^{1,4,5} , Bogdan Ștefan Vasile^{3,6,7} , Ecaterina Andronescu^{1,4,*} , Florica Marinescu^{4,6} and Alina Maria Holban^{3,4,6}

- ¹ Department of Science and Engineering of Oxide Materials and Nanomaterials, Faculty of Applied Chemistry and Materials Science, University Politehnica of Bucharest, 011061 Bucharest, Romania; delia_albulet@yahoo.com (D.A.); ada_birca@yahoo.com (A.C.B.); anton_ficai81@yahoo.com (A.F.); grumezescu@yahoo.com (A.M.G.)
 - ² Department of Preclinical Sciences, Faculty of Veterinary Medicine, University of Agronomic Sciences and Veterinary Medicine of Bucharest, 105 Blvd. Splaiul Independentei, 050097 Bucharest, Romania; floriniordache84@yahoo.com
 - ³ National Research Center for Micro and Nanomaterials, University Politehnica of Bucharest, 060042 Bucharest, Romania; bogdan.vasile@upb.ro (B.Ș.V.); alina.m.holban@bio.unibuc.ro (A.M.H.)
 - ⁴ Research Institute of the University of Bucharest—ICUB, University of Bucharest, 050657 Bucharest, Romania; florica.marinescu@bio.unibuc.ro
 - ⁵ Academy of Romanian Scientists, Ilfov Str. No. 3, 50044 Bucharest, Romania
 - ⁶ Department of Microbiology and Immunology, Faculty of Biology, University of Bucharest, 91-95 Splaiul Independentei Street, 077206 Bucharest, Romania
 - ⁷ Research Center for Advanced Materials, Products and Processes, University of Bucharest, 060042 Bucharest, Romania
- * Correspondence: ecaterina.andronescu@upb.ro



Citation: Stoica, A.E.; Albuleț, D.; Bîrcă, A.C.; Iordache, F.; Ficăi, A.; Grumezescu, A.M.; Vasile, B.Ș.; Andronescu, E.; Marinescu, F.; Holban, A.M. Electrospun Nanofibrous Mesh Based on PVA, Chitosan, and Usnic Acid for Applications in Wound Healing. *Int. J. Mol. Sci.* **2023**, *24*, 11037. <https://doi.org/10.3390/ijms241311037>

Academic Editor: Xiao Hu

Received: 19 April 2023

Revised: 23 June 2023

Accepted: 24 June 2023

Published: 3 July 2023



Copyright: © 2023 by the authors. Licensee MDPI, Basel, Switzerland. This article is an open access article distributed under the terms and conditions of the Creative Commons Attribution (CC BY) license (<https://creativecommons.org/licenses/by/4.0/>).

Abstract: Injuries and diseases of the skin require accurate treatment using nontoxic and noninvasive biomaterials, which aim to mimic the natural structures of the body. There is a strong need to develop biodevices capable of accommodating nutrients and bioactive molecules and generating the process of vascularization. Electrospinning is a robust technique, as it can form fibrous structures for tissue engineering and wound dressings. The best way of forming such meshes for wound healing is to choose two polymers that complement each other regarding their properties. On the one hand, PVA is a water-soluble synthetic polymer widely used for the preparation of hydrogels in the field of biomedicine owing to its biocompatibility, water solubility, nontoxicity, and considerable mechanical properties. PVA is easy to subject to electrospinning and can offer strong mechanical stability of the mesh, but it is necessary to improve its biological properties. On the other hand, CS has good biological properties, including biodegradability, nontoxicity, biocompatibility, and antimicrobial properties. Still, it is harder to electrospin and does not possess as good mechanical properties as PVA. As these structures also allow the incorporation of bioactive agents due to their high surface-area-to-volume ratio, the interesting point was to incorporate usnic acid into the structure as it is a natural and suitable alternative agent for burn wounds treatment which avoids an improper or overuse of antibiotics and other invasive biomolecules. Thus, we report the fabrication of an electrospun nanofibrous mesh based on PVA, chitosan, and usnic acid with applications in wound healing. The obtained nanofibers mesh was physicochemically characterized by Fourier transform infrared spectroscopy (FT-IR) and scanning electron microscopy (SEM). In vitro biological assays were performed to evaluate the antimicrobial properties of the samples using the MIC (minimum inhibitory concentration) assay and evaluating the influence of fabricated meshes on the *Staphylococcus aureus* biofilm development, as well as their biocompatibility (demonstrated by fluorescence microscopy results, an XTT assay, and a glutathione (GSH) assay).

Keywords: electrospinning; nanofibers; wound healing; PVA; chitosan; usnic acid

1. Introduction

Over the past decades, nanotechnology has been providing novel technologies which enable the manufacturing of nanomaterials with unique properties for various applications [1–4]. One of the most simple, versatile, and effective fabrication methods used in nanotechnology since 1990 is represented by the electro-hydrodynamic (EHD) technique named electrospinning. Since then, substantial progress has been made in the design of the instrument, processing materials, and final products [5–7]. Over the past years, the amount of research on electrospun nanofibrous materials for potential ecological, electronic [8–11], biological, and biomedical applications has increased exponentially [5,6,12–14]. This procedure enables the fabrication of nanofibers of sizes ranging from tens of nanometers or microfibers that present diameters of hundreds of micrometers by using a simple principle and an easily controllable apparatus [12,13,15–17]. An important advantage of electrospinning is that the morphology, internal structure, sizes, architectures, and surface properties are tunable and controllable, making this technique eligible for various investigations and applications in the biomedical field. Owing to these suitable characteristics, electrospinning has shown a great potential to obtain products with improved and innovative facilities in tissue engineering [18–22], wound dressings [23–26], drug delivery systems [19,27–31], biosensors [30,32,33], healthcare products [34–36], etc.

The most important parameters that influence the fibers' characteristics are (i) the processing parameters, such as solution feeding rate, needle diameter, rotating speed of the collector, and applied voltage; (ii) the solution properties, such as the polymer's molecular weight, concentration [15], conductivity, and viscosity; and (iii) the environmental factors such as humidity and temperature. These factors have an important influence on the morphology and structure of fibers [12,37,38].

Due to their characteristics, polymers are great candidates that provide special features to the fabricated nanofibers or scaffolds. About 100 different polymers have already been used for electrospun nanofibers fabrication [12,15,37,39].

Polyvinyl alcohol (PVA) belongs to the category of water-soluble synthetic polymers, being a good candidate for the preparation of hydrogels [40–43] and widely used in the field of biomedicine [44,45] due to its suitable characteristics such as its biocompatibility, water solubility, nontoxicity, and considerable mechanical properties [41,46,47]. Other uses are related to textiles, papermaking, and coatings [48,49]. Among the properties that make PVA interesting for various applications are easy preparation, good adhesive, and emulsifying properties, a film-forming ability, important mechanical stability, outstanding chemical resistance, and high barrier properties for oxygen and odor [50].

Chitosan (CS) presents impressive biological properties, including biodegradability, nontoxicity, biocompatibility, and antimicrobial properties, promoting pain relief and blood clotting [51], which make it eligible for biomedical applications [52–55]. The CS structure of nanofibers mimics the natural ECM of the skin and boosts the healing process [46,56]. Electrospinning of CS presents some limitations due to its polycationic nature in solution, as forming solid hydrogen bonds constrains the free motility of the polymeric chain. In contrast, repulsive forces among ionic groups avoid creating enough chain entanglements [46,57–60].

Usnic acid (UA) has been widely researched in the field of healthcare, being a useful agent in burns and wound therapies [61,62]. Studies showed that UA has an antimicrobial effect against anaerobic bacteria such as *Bacteroides ruminicola* ssp. *Brevis*, *Bacteroides fragilis*, *Bacteroides vulgatus* [63,64], *Clostridium perfringens* [63–65], *Propionibacterium acnes* [63–65], *Bacteroides thetaio-micron* [63,64], Gram-positive bacteria such as *Enterococcus faecium* [63,64], *Enterococcus faecalis* [63–65], *Staphylococcus aureus* [64–67], *S. mutans* [68–71], *S. epidermidis* [63,65,72], *Streptococcus pyogenes* [63,64,73,74], *Streptococcus pneumoniae* [64,65], Gram-negative bacteria such as *Escherichia coli*, *Haemophilus influenzae*, *Pseudomonas aeruginosa*, and Mycobacteria such as *M. aurum*, *M. avium*, *M. smegmatis*, *M. tuberculosis* var. *bovis*, *M. tuberculosis* var. *hominis* [64]. Although all these properties make it suitable as a wound-healing agent, there are some limitations in terms of its low water solubility that researchers have tried to over-

come by using more soluble salt forms, encapsulating them into liposomes in collagen and gelatin films, including them into β -cyclodextrins, or encapsulating them in electrospun fibers [61].

The purpose of this study was to design and characterize an electrospun nanofibrous mesh based on polyvinyl alcohol, chitosan, and usnic acid with applications in wound healing. The obtained nanofibers are physicochemically characterized using Fourier transform infrared spectroscopy (FT-IR) and scanning electron microscopy (SEM). In vitro biological assays are performed in order to evaluate the antimicrobial properties of the samples, as well as their biocompatibility using fluorescence microscopy, an XTT assay, and a glutathione (GSH) assay.

2. Results and Discussions

In the past 20 years, electrospinning has grown significantly as a micro- and nanofiber processing method. It continues to represent the most effective method to produce them in a variety of designs for tissue engineering and regenerative medicine, providing modern and efficient solutions for current day-to-day challenges [75–78].

2.1. Fourier Transform Infrared Spectroscopy (FT-IR)

To investigate the composition of the obtained electrospun materials (by identifying the characteristic absorption bands and the interactions between compounds), FT-IR spectra were recorded for the 5%PVA_2%CS and 5%PVA_2%CS-UA nanofibers. In Figure 1, the spectra of raw materials and prepared samples are presented. The absorption band at 3271.67 cm^{-1} corresponds to the O-H stretching and the intramolecular hydrogen bonds of PVA [79–81]. An absorption band can be observed at around 2907.87 cm^{-1} and can be attributed to C-H symmetric and asymmetric stretch vibrations for both PVA and CS [79,81]. The peak available at 1645 cm^{-1} can be assigned to the C=O stretching of amide I, and the peak at 1325 cm^{-1} can be assigned to the C-N stretching of amide III, both characteristic of the residual N-acetyl groups from chitosan. Moreover, 1589 cm^{-1} corresponds to the N-H bending of the primary amine [82]. The peak depicted at 1418.97 cm^{-1} can be assigned to the CH_3 symmetrical deformation vibration of PVA.

The presence of the H-C-O groups of PVA was confirmed by the bands at around 1073.01 cm^{-1} , which could also be assigned to the C-O stretching vibration of CS. Characteristic peaks at around 834.82 cm^{-1} are related to the saccharide structure of CS. In the band interval ranging from 515.97 cm^{-1} to 469.60 cm^{-1} , the C-C skeleton vibration of PVA can be found [80,83–85]. No relevant IR bands characteristics of UA were identified in the fibrous mats due to the fact that the amount of UA present in the samples was under the detection limit of the ATR equipment. The UA presence in the sample was further confirmed by the antimicrobial evaluation.

2.2. Scanning Electron Microscopy (SEM)

SEM micrographs showed relevant information regarding the morphology and topography of both simple (5%PVA_2%CS-UA) and usnic acid-incorporated nanospun (5%PVA_2%CS-UA) microfiber meshes. Figure 2 displays the micrographs of the mesh containing PVA and CS. The nanofibrous architecture can be clearly observed, and the formation of an entangled structure of nanofibers was confirmed. Nanofibers with diameters ranging from 14.86 nm to 75.06 nm with predominant sizes between 30 and 40 nm were formed in a nonwoven assembly, having a linear shape and being organized with a random orientation. The images exposed fibers with ramifications that formed a highly porous structure suitable for their application in wound healing, as it resembled the natural ECM.

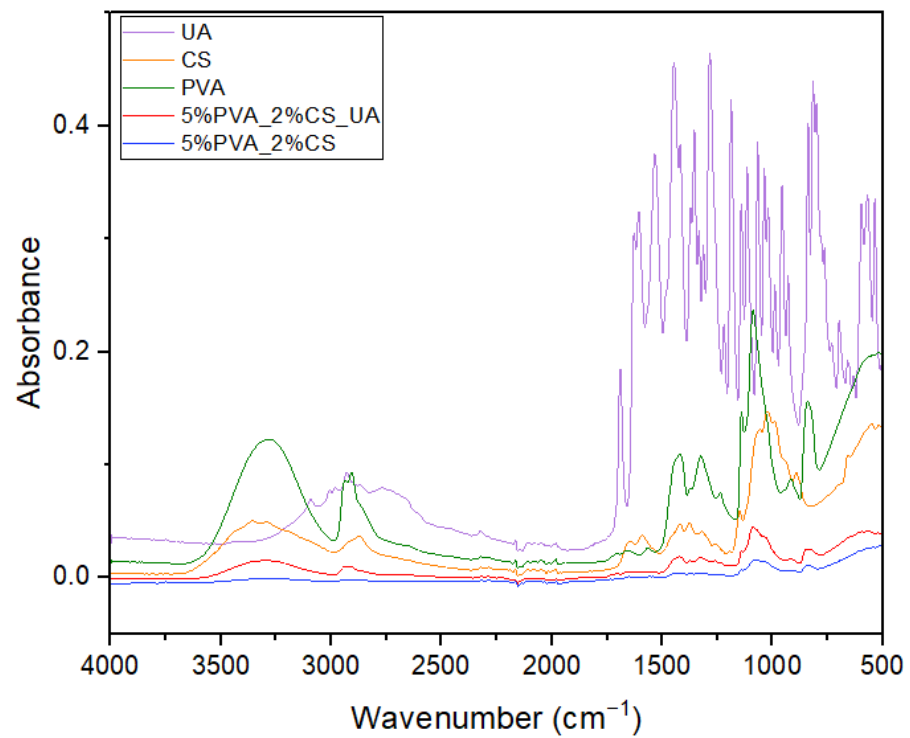


Figure 1. FT-IR spectra of PVA, CS, UA, and 5%PVA_2%CS and 5%PVA_2%CS_UA electrospun nanofiber meshes.

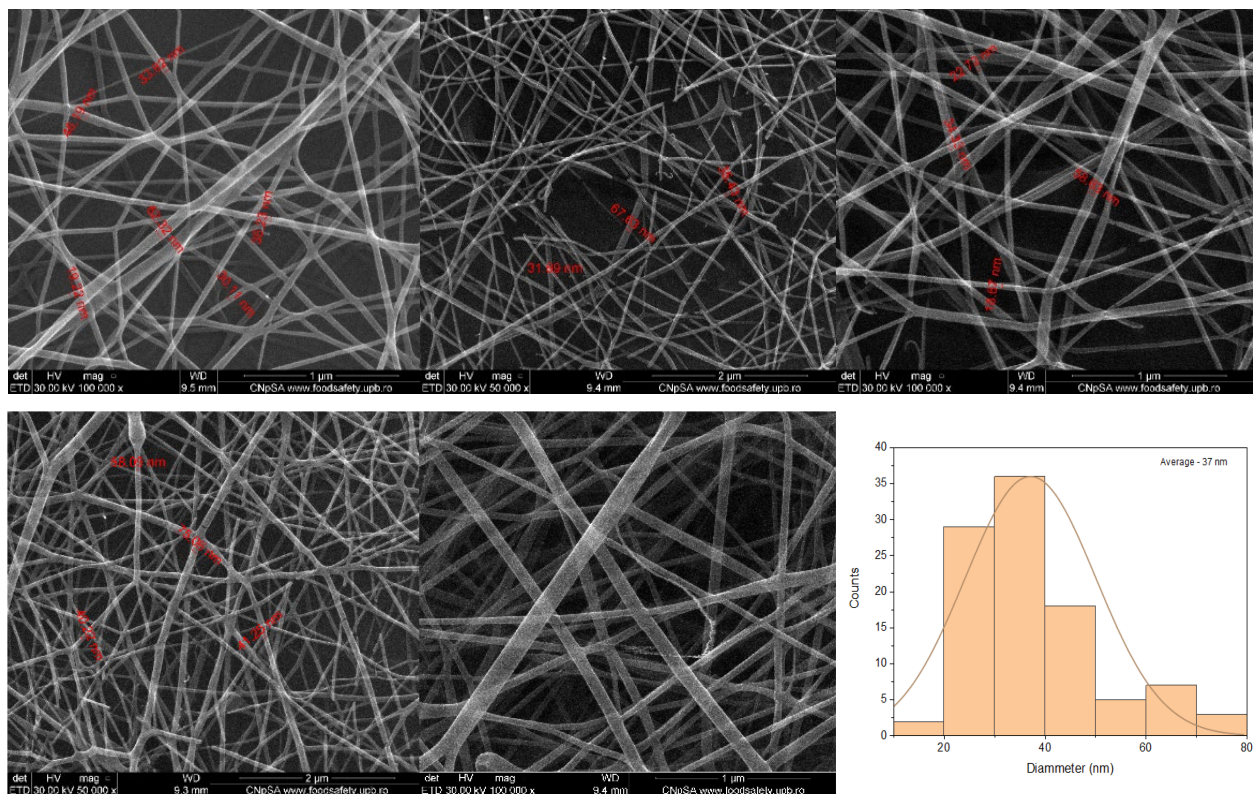


Figure 2. SEM images of electrospun nanofibers obtained for the 5%PVA_2%CS nanofiber mesh.

Figure 3 presents the morphology of the PVA and CS mesh with usnic acid (5%PVA_2%CS_UA), confirming the successful construction of a nanofibrous structure. The nanofibers' diameter size was between 28 nm and 203.2 nm, with average values at 60–80 nm. It is visible that

the nanofiber size increased by introducing usnic acid into the system. However, all other properties, such as the high porosity degree and good structural integrity, remained the same for the simple mesh. These nanofibers were also arranged in a nonwoven assembly. Fibers were smooth and continuous, being arranged in a disordered manner.

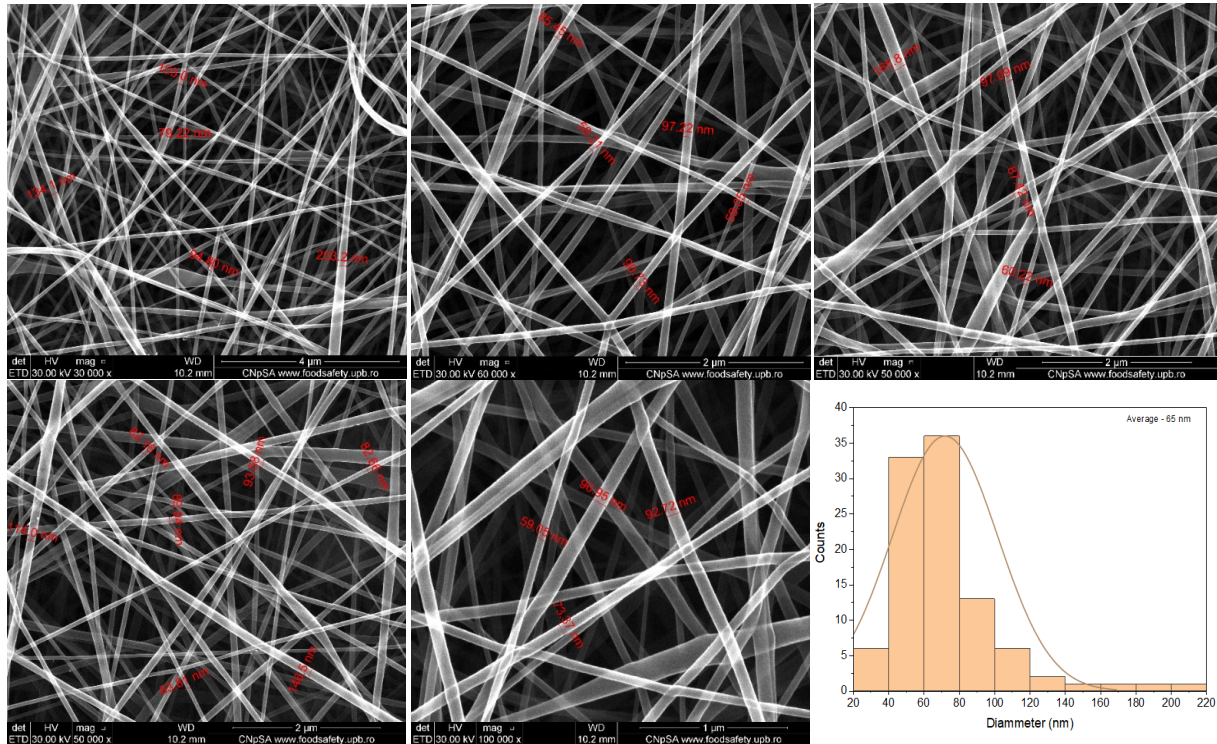


Figure 3. SEM images of electrospun nanofibers obtained for the 5%PVA_2%CS-UA nanofiber mesh.

2.3. Stability Tests

To mimic the stability of the 5%PVA_2%CS and 5%PVA_2%CS-UA fibrous mats in physiological fluids, the samples were immersed in a simulated fluid of blood plasma obtained according to Kokubo's method [86], termed simulated blood fluid (SBF), and also in phosphate buffer (PBS). As can be observed in Figure 4, the SEM images revealed a good interaction of SBF and PBS with the fibrous mats, highlighting that on the surface of the samples, mineral deposits appeared. Moreover, no fibrillar structures were available due to the ability of the tested mats to swell in various aqueous environments.

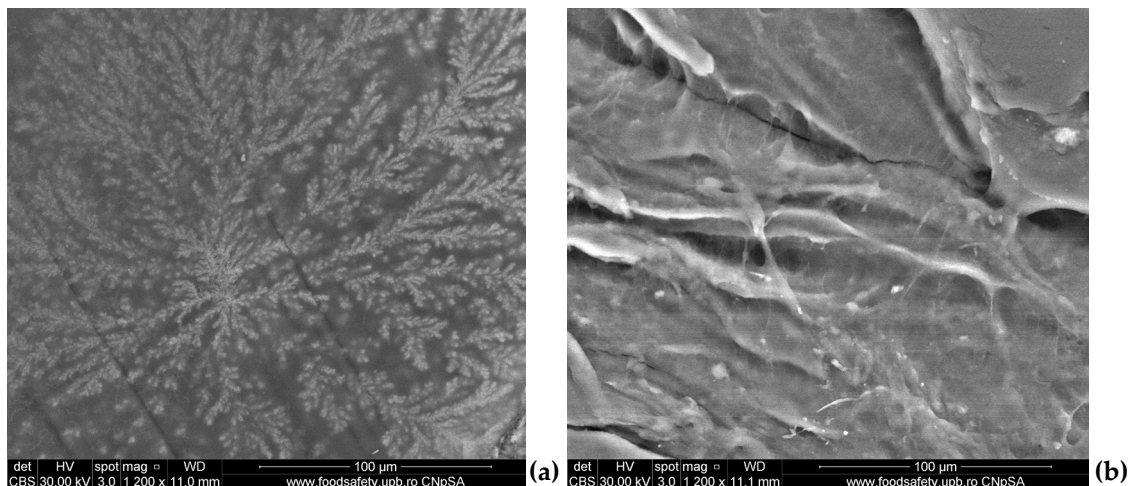


Figure 4. SEM images of fibrous mats (without UA) after immersion in: (a) SBF for 72 h, (b) PBS for 72 h.

2.4. XTT Assay

The XTT test graph shown in Figure 5 delivers information about the cell viability after exposure to the 5%PVA_2%CS and 5%PVA_2%CS-UA samples at 24 h, 48 h, and 72 h. Both samples presented good biocompatibility; the cell viability degree was above 90% at all three measurement times. After the first 24 h, there were no significant changes, showing that the two materials had similar values to the control. After 48 h, there was an increase in cell viability for the 5%PVA_2%CS sample, which exceeded the control values. However, after 72 h, a considerable decrease could be registered, which implied that the material without usnic acid did not have a proliferative effect on cells.

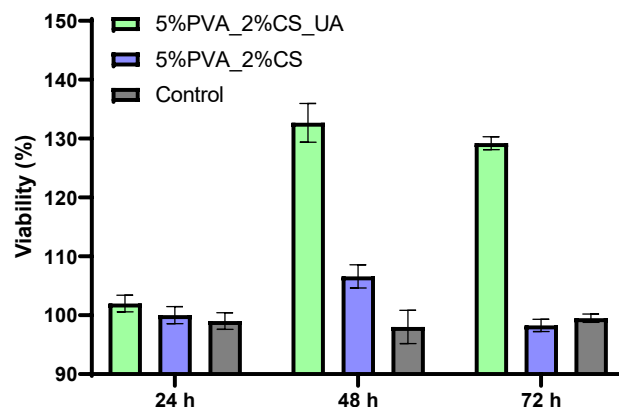


Figure 5. XTT assay after exposure of cells to the 5%PVA_2%CS-UA and 5%PVA_2%CS nanofibers mesh.

Nevertheless, the PVA/CS mesh with usnic acid incorporated (5%PVA_2%CS-UA), showed extraordinary results after 48 h and 72 h, increasing the cell viability by almost 30% compared to that of the control. This fact confirmed the suitable biocompatibility of the electrospun mesh with usnic acid and made the material eligible as a proper biodevice that sustains the proliferation and growth of cells. Moreover, these findings support previous studies that indicated the protective role of usnic acid in endothelial cells by exhibiting analgesic, antipyretic, and anti-inflammatory characteristics [87,88].

2.5. Glutathione (GSH) Assay

The oxidative stress of AFSC was evaluated by the amount of glutathione existing for the 5%PVA_2%CS and 5%PVA_2%CS-UA nanofiber meshes versus the control, as shown in Figure 6. Both 5%PVA_2%CS and 5%PVA_2%CS-UA meshes exhibited a glutathione amount comparable with that of the control, the differences being statistically insignificant. Therefore, results indicated that in contact with the AFSC, the materials did not stimulate the occurrence of oxidative stress. High levels of GSH are correlated with cellular damage and are very important in order to assess the level of cellular stress that can potentially lead to apoptosis and cell death.

2.6. Fluorescence Microscopy

AFSC cultivated in the presence of 5%PVA_2%CS and 5%PVA_2%CS-UA were observed by fluorescence microscopy, as shown in Figure 7. The high number of viable (red) cells demonstrated the biocompatibility of the fabricated fibrous mats [87]. Cellular morphology was compared with control cells. The AFSC cultivated with nanofibrous meshes presented a normal fibroblast-like phenotype. The AFSC presented a good attachment to the substrate compared with the control, with the integrity of the cellular membrane and a low number of vacuoles, suggesting that the nanofibrous meshes did not exhibit a cytotoxic effect. Additionally, studies [89] have shown that the process triggered by usnic acid does not include DNA damage, indicating that usnic acid is not a genotoxic compound.

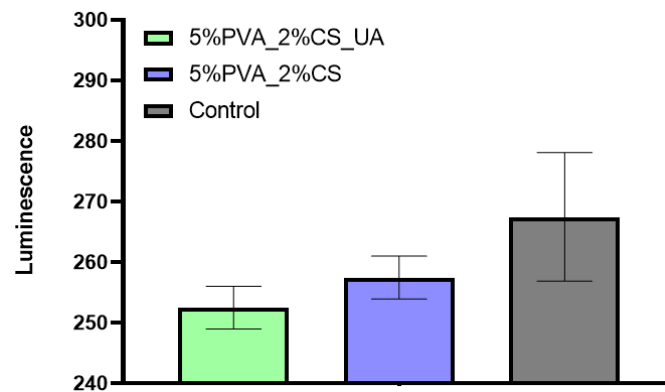


Figure 6. GSH Assay for AFSC after being in contact with the 5%PVA_2%CS and 5%PVA_2%CS_UA meshes.

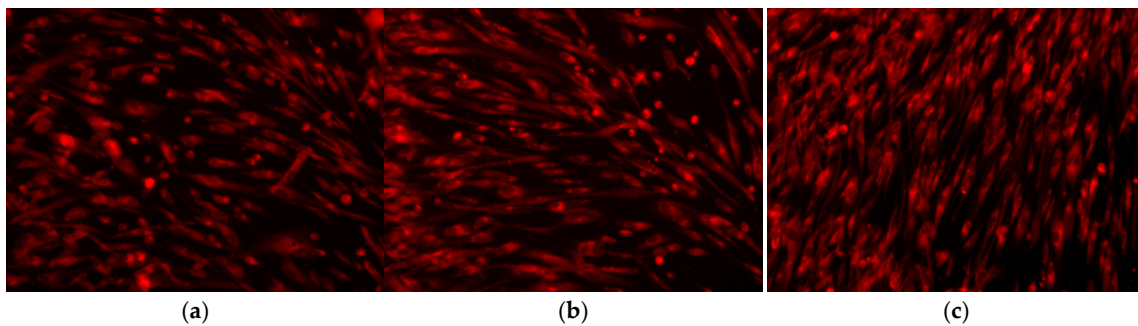


Figure 7. Fluorescence micrographs for (a) 5%PVA_2%CS mesh; (b) 5%PVA_2%CS_UA mesh, and (c) control.

2.7. Effect of Nanostructured Meshes on Biofilm Production

Many serious and resistant infections in hospitalized patients are caused by the opportunistic pathogen *S. aureus*. The growth curve graph shown in Figure 8 presents the CFU/mL versus incubation time at 24 h, 48 h, and 72 h for *S. aureus* treated with the 5%PVA_2%CS_UA mesh. Data represent the mean values of two determinations performed at each time point. It is visible that the 5%PVA_2%CS_UA mesh managed to have an improved anti-biofilm activity, showing lower rates of CFU/mL than the control. However, it is noticeable that in time, this activity decreases.

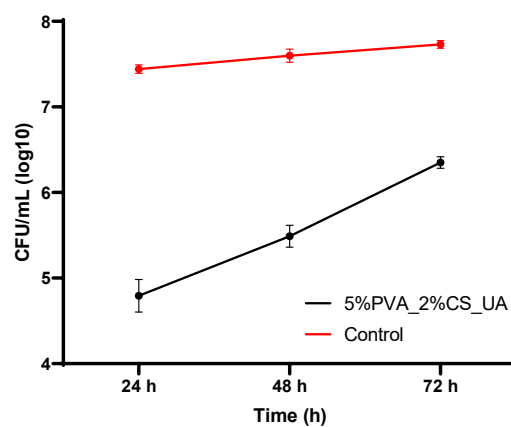


Figure 8. The mean value of log₁₀ CFU (colony-forming units)/mL of *S. aureus* recorded at 24 h, 48 h, 72 h for the 5%PVA_2%CS_UA mesh compared to the control.

However, as Figure 6 reveals, the anti-biofilm effect was maintained for at least 72 h against *S. aureus*, cultured in standard conditions. The biofilm inhibition could be

evaluated by the release of active UA contained in the prepared nanofiber meshes, a natural compound that has been previously reported to act as an antimicrobial agent against Gram-positive species such as *S. aureus* [87,90–94] and *E. faecalis* [92] and Gram-negative species such as *P. aeruginosa* and *E. coli* [92]. The ability of usnic acid to interfere with the growth and biofilm formation of *S. aureus* constitutes an important aspect in developing alternative antistaphylococcal therapies containing natural compounds. Compared to conventional antibiotics, these medicines have the significant advantage of being less toxic and preventing the spread of bacteria that are resistant to treatment [87].

Over the past decades, many developments have focused on fabricating ECM-like scaffolds made of nanofibers through electrospinning because of their unique morphology, high surface-area-to-volume ratio, and porosity [95,96]. ES-fabricated biostructures provide good assistance for various tissue types regarding regeneration and reconstruction, namely, they are able to mimic the natural ECM and initiate special biological responses, accelerating the attachment and stimulating cell growth, proliferation, and differentiation [24,97].

Given the very good reaction of PVA in contact with the biological environment and its ability to significantly absorb high quantities of water or biological fluids without dissolving, it means that the best solution is to blend PVA with other polymers to obtain a favorable wound dressing that highlights the advantages of both polymers [50]. At the same time, CS is more suitable to be electrospun with other polymers in order to efficiently develop the properties of the fibers [98–102]. The selection of a flexible polymer in combination with CS, such as PVA, can be chosen in order to improve the electrospinning of chitosan and the properties of the end product [57,103–105]. One important factor in the design of CS-based biomaterials is represented by the mechanisms of its degradation in the biological environment [106]. Numerous synthesis methods have been studied to create CS, which degrades over days, weeks, or even months, depending on the needs of the specific application or biodevice [105–108]. Furthermore, studies [109–112] reported that by adding bioactive components to functionalized nanomaterials, accelerated healing was achieved by regulating the metabolic pathway and growth factors. Usnic acid (UA), a dibenzofuran produced from lichen, is one of them [113]. Usnic acid is able to reduce the inflammation related to burns and to encourage wound closure through keratinocyte monolayers [64,114].

Herein, composite PVA/CS and PVA/CS/UA nanofibrous scaffolds were developed by electrospinning, and their antimicrobial properties, as well as their biocompatibility, were demonstrated using fluorescence microscopy, an XTT assay, and a glutathione (GSH) assay.

On the one hand, the large surface area and pore volume ratio and uniform and well-structured porosity of the fiber mat allowed the wound exudates absorption while reducing the potential bacterial infection [115]. As a general remark, the SEM images recorded for both samples exposed macroporous fibrous networks with ramifications that formed a highly porous structure, uniformly distributed and randomly oriented defect-free fibers with diameters ranging from 14.86 nm to 203.3 nm, suitable for their application in wound healing, as it resembled the natural ECM [116,117]. To mimic the stability of fibrous mats in physiological fluids, the samples were immersed in simulated body fluid (SBF) and also in phosphate buffer (PBS), respectively. The SEM images revealed a good interaction of SBF and PBS with fibrous mats, underlining that on the surface of samples, mineral deposits became visible. Furthermore, no fibrillar structures could be observed due to the ability of the tested mats to swell in different aqueous environments. It is important to mention that the swelling ability of the PVA/CS fibers represents an important property that characterizes the utilization of the mats for wound dressing applications [118].

On the other hand, given that cell viability was above 90% at each of the three measurement times, both samples exhibited good biocompatibility. There were no noticeable changes after the first 24 h, indicating that the two materials exhibited values that were comparable to those of the control. Furthermore, it was noticed that in contact with the AFSC, the fibrous materials did not promote the occurrence of oxidative stress. High levels of GSH are linked to cellular damage and are highly significant in order to evaluate the

level of cellular stress that can potentially lead to apoptosis and cell death. Moreover, the high number of viable cells demonstrated the biocompatibility of the fabricated fibrous structures (Figure 7).

Last but not least, because an important part of serious and resistant infections in hospitalized patients is induced by the opportunistic pathogen *S. Aureus* [119], the 5%PVA_2%CS_AU mesh was evaluated in order to assess the effect of the nanostructured meshes on biofilm production. The results proved that the mesh presented an improved anti-biofilm activity, demonstrating lower rates of log CFU/mL than those of the control; however, it was clear that, in time, this activity decreased.

Thus, the developed fibrous mats based on PVA/CS/UA hold great promise in wound-healing applications.

3. Materials and Methods

3.1. Materials

Polyvinyl alcohol (PVA, $(C_2H_4O)_n$, 99% hydrolyzed), chitosan (CS, medium molecular weight, 75–85% deacetylation degree), and usnic acid (98% purity) were purchased from Sigma-Aldrich (Merck Group, Darmstadt, Germany). All the reagents were analytical grade and used without any further purification.

3.2. Preparation Methods and Electrospinning Parameters

In the first stage, two solutions of 5%PVA and 2%CS were prepared. Thus, a first solution of 5%PVA (Mw) in water was prepared. The solution was maintained at 80 °C under gentle stirring for 1 h, followed by ultrasonication. Then, a second 2%CS solution was made using aqueous acetic acid 1N at room temperature under gentle stirring for 1 h to form a homogeneous solution, which was subjected to ultrasonication as well.

The electrospinning process (Figure 9) was carried out using a Tong Li Tech nanofiber electrospinning unit at room temperature. The device is composed of a syringe pump, a high-voltage DC power supply, a spinning polymer solution, and a rotating cylindrical collector.

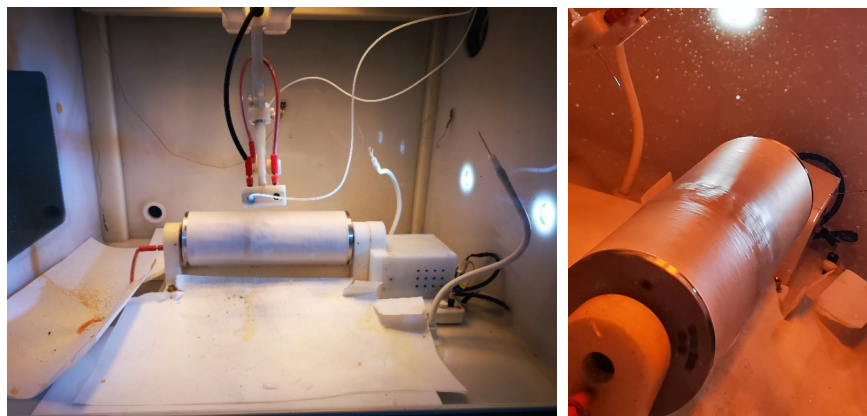


Figure 9. Electrospinning process. The solutions are expelled in jets through the syringe and form nanofibers on the rotating collector.

Thus, for the sample containing PVA and CS (named 5%PVA_2%CS), 5 mL of solution 1 (5%PVA) and 5 mL of solution 2 (2%CS) were mixed and loaded into a polypropylene syringe connected to an 18-gauge blunt-end needle and then mounted on a digital syringe pump. The electrospinning procedure was carried out using the specific operation parameters shown in Table 1. The needle-to-target distance was 120 mm. The fibers were directly deposited on a piece of grounded aluminum foil.

Table 1. Electrospinning Operating Parameters.

Parameters	Solutions	
	5%PVA_2%CS	5%PVA_2%CS-UA
Flow rate, mL/h	3–7	5
Output voltage, KV	–6 -> –3	–6.5
Fan speed, rpm	17 -> 20	17
Humidity degree, %	80	80
Temperature, °C	~20	~20
Heater output, KW	~28	~28
	0.6	0.6

In order to obtain a nanofiber mesh based on PVA, chitosan and usnic acid (named 5%PVA_2%CS-UA), solution 1 (5%PVA) and solution 2 (2%CS) were prepared through the same method as previously described. Additionally, a third solution of 1% usnic acid in dimethyl sulfoxide (DMSO) was prepared. Further, 4.5 mL of solution 1 (5%PVA) together with 4.5 mL of solution 2 (2%CS) and 1 mL of solution 3 (1% usnic acid) were mixed and loaded into a polypropylene syringe connected to an 18-gauge blunt-end needle and then mounted on a digital syringe pump. The electrospinning deposition was carried out under the operating conditions described in Table 1. The needle-to-target distance was 120 mm. The fibers were directly deposited on a piece of grounded aluminum foil.

3.3. Physicochemical Characterization

3.3.1. Fourier Transform Infrared Spectroscopy (FT-IR)

Infrared spectroscopy is a useful technique that can offer valuable information about interactions in polymer blends, confirming the integrity of functional groups characteristic of the synthesized materials. FT-IR spectra were recorded using the Nicolet 6700 FT-IR spectrometer, purchased from Thermo Nicolet (Madison, WI, USA). A small amount of particulate suspension was analyzed by a ZnSe crystal, and measurements were carried out through 32 sample scans between 4000 and 500 cm^{-1} at a resolution of 4 cm^{-1} at room temperature. In order to be able to register the acquired information, the spectrometer was connected to a data acquisition and processing unit through the Omnic program (version 8.2 Thermo Nicolet).

3.3.2. Scanning Electron Microscopy (SEM)

The morphological analyses of the two materials were carried out using scanning electron microscopy. For this purpose, a scanning electron microscope purchased from the FEI Company (Hillsboro, OR, USA) was used. The samples were shaped with a diamond disc and fixed on a sample support to be introduced into the analysis zone. The shape and size of the PVA/CS nanofibers of the mesh were determined through micrographs of the samples by direct measurements of the resulting secondary electron beam with a 30 keV energy at different points of the samples.

3.3.3. Stability Tests

In order to assess the interactions among the obtained fibrous mats (cut in a square shape of 1/1 cm), the samples were immersed in simulated blood fluid (SBF) obtained according to Kokubo's method [86] and in phosphate buffer (PBS) as well. For 72 h, the fibrous materials were subjected to physiological conditions at 37 °C. After that, qualitative analysis by SEM was performed.

3.4. In Vitro Biocompatibility

3.4.1. XTT Assay

The biocompatibility of the synthesized nanofibrous mesh samples was evaluated using an XTT reagent (2,3-Bis-(2-Methoxy-4-Nitro-5-Sulphophenyl) -2H-Tetrazolium- 5-Carboxanilide) according with the manufacturer protocol (CyQUANT™ XTT Cell Viability Assay Kit,

Thermo Fischer Scientific, Waltham, MA, USA). The assay kit included the XTT reagent and an electron-coupling reagent. The XTT reagent is a tetrazolium-based compound sensitive to cellular redox potential. Actively viable cells convert the water-soluble XTT compound to an orange-colored formazan product. The sensitivity and consistency of the assay are significantly increased when used with the electron-coupling reagent. The human mesenchymal amniotic fluid stem cells (AFSC) were grown in DMEM (Sigma-Aldrich, Saint Louis, MO, USA) supplemented with 10% fetal bovine serum, 1% antibiotics (penicillin and streptomycin) (Sigma-Aldrich, Saint Louis, MO, USA), changed twice a week. The AFSC were placed in 96-well plates, at a density of 3000 cells/well, in the presence of nanofibrous mesh for 24 h, 48 h, and 72 h. The control samples were represented only by AFSC cultivated in the same condition but without the nanofibrous mesh. Subsequently, 70 μ L of XTT solution was added to the cells, followed by incubation at 37 °C for 4 h. After a vigorous homogenization of the formazan crystals, the absorbance was read at 450 nm using a TECAN Infinite M200 spectrophotometer (Männedorf, Switzerland).

3.4.2. GSH-Glo Glutathione Assay

The oxidative stress was assessed using the GSH-Glo glutathione assay kit (Promega, Madison, WI, USA). AFSC was seeded at a density of 3000 cells in 300 μ L DMEM supplemented with 10% fetal bovine serum and 1% antibiotics (penicillin, streptomycin/neomycin) in 96-well plates. After 24 h of seeding, AFSC was put in contact with the nanofibrous mesh and then incubated for another 24 h. Furthermore, 100 μ L of 1X GSH-Glo reagent was added, followed by an incubation at 37 °C for 30 min, followed by 100 μ L of luciferin detection reagent and an incubation at 37 °C for an additional 15 min. The medium from the cell cultures was well homogenized, and then the plate was read on the luminometer (Microplate Luminometer Centro LB 960, Berthold, Germany).

3.4.3. Fluorescence Microscopy

For the evaluation of cellular biocompatibility in terms of cellular shape, attachment to the substrate, the integrity of the cellular membrane, and the number of vacuoles, we used fluorescence microscopy and a red CMTPX fluorophore (Thermo Fischer Scientific, Waltham, MA, USA). The CMTPX is a cell tracker for the long-term tracing of living cells, which, when entered into the cells, start to emit fluorescence. The viability and morphology of the AFSC were evaluated after 5 days of cultivation of the AFSC in the presence of the nanofibrous mesh. The CMTPX fluorophore was added to the cell cultures at a concentration of 5 μ M and incubated for 30 min. Finally, the AFSC cultures were washed with PBS and visualized by fluorescent microscopy using an Olympus CKX 41 digital camera driven by CellSense Entry software (Olympus, Tokyo, Japan).

3.4.4. Anti-Biofilm Effect

To test the effect of the nanostructured meshes on the biofilm production, samples were sterilized by exposure to UV radiation for 20 min on each side. A 0.5 cm/0.5 cm sample of the material was individually deposited in a well of a 6-well sterile plate. Over the deposited materials, 2 mL of liquid medium was added to the wells, followed by 50 μ L of 0.5 McFarland microbial suspension. The 6-well plates thus prepared were incubated at 37 °C for 24 h. After incubation, the materials were washed with PBS (phosphate-buffered saline), and the medium was changed to allow biofilm development. Plates were incubated for different periods (24 h, 48 h, 72 h). Upon expiration of the incubation period, the sample on which the biofilm was developed was washed with PBS and placed in a sterile tube containing 1 mL of PBS. The tube was vortexed vigorously for 30 s to detach the cells from the developed biofilm. The obtained cell suspension was diluted, and various dilutions were seeded on solidified culture media plates to obtain and quantitate the number of colony-forming units per mL.

4. Conclusions

Electrospinning offers a robust and versatile technique to produce 2D and 3D nanofiber meshes with patterned and porous structures. Numerous opportunities in the field of biomedicine have opened up thanks to the biomimicry that these structures offer, including in scaffolds, drug delivery, cell behavior control, and regenerative medicine. Incorporating bioactive molecules into electrospun nanofiber meshes represents a beneficial development in wound healing because these hybrid structures positively affect wounds and can initiate and accelerate the healing process. This study presented the preparation and characterization of an electrospun nanofiber mesh based on polyvinyl alcohol, chitosan, and usnic acid with applications in wound healing. The physicochemical characterization revealed a fibrous structure with fiber dimensions ranging from 14.86 nm to 75.06 nm with predominant sizes between 30 and 40 nm. SEM images showed a nonwoven assembly having a linear shape with a random orientation. The images exposed fibers with ramifications that formed a highly porous structure suitable for their application in wound healing because it mimicked the natural ECM. The XTT assay showed extraordinary results after 48 h and 72 h for 5%PVA_2%CS-UA, increasing the cell viability by almost 30% compared to that of the control. This fact confirmed the suitable biocompatibility of the electrospun mesh with usnic acid and made the material eligible as a proper biodevice that sustains the proliferation and growth of cells. The cell viability revealed using fluorescent microscopy was comparable with that of the control, meaning that the nanofiber meshes did not exhibit a cytotoxic effect. From the point of view of biofilm development, the 5%PVA_2%CS-UA presented an improved anti-biofilm activity against the *S. aureus* strain. In conclusion, all these results affirm that electrospun nanofibers mesh based on PVA, chitosan, and usnic acid could be a promising material for applications in wound healing.

Author Contributions: Conceptualization, A.M.G., A.E.S. and E.A.; methodology, E.A., F.I., A.M.H., A.F. and A.M.G.; validation, A.M.G. and E.A.; synthesis, A.E.S., A.C.B. and D.A.; formal analysis, A.E.S., A.C.B., A.M.G., F.I., A.M.H., B.S.V., F.I. and F.M.; investigation, A.E.S., A.C.B., A.M.G., B.S.V., F.I., A.F., F.M. and A.M.H.; writing—original draft preparation, A.E.S. and D.A.; writing—review and editing, A.E.S., A.M.G. and D.A.; supervision, E.A. and A.M.G. All authors have read and agreed to the published version of the manuscript.

Funding: This work was supported by the grant POCU/993/6/13 -153178, cofinanced by the European Social Fund within the Sectorial Operational Program Human Capital 2014–2020 and Romanian Government through the national program “Installations and Strategic Objectives of National Interest”.

Institutional Review Board Statement: Not applicable.

Informed Consent Statement: Not applicable.

Data Availability Statement: Not applicable.

Conflicts of Interest: The authors declare no conflict of interest.

References

1. Grumezescu, A.M. *Nanomaterials for Drug Delivery and Therapy*; William Andrew: Norwich, NY, USA, 2019.
2. Stoica, A.E.; Chircov, C.; Grumezescu, A.M. Nanomaterials for wound dressings: An up-to-date overview. *Molecules* **2020**, *25*, 2699. [[CrossRef](#)]
3. Gogotsi, Y. *Nanomaterials Handbook*; CRC Press: Boca Raton, FL, USA, 2006.
4. Tuah, K.A.; Chin, S.F.; Pang, S.C. Fabrication of Drug-Loaded Starch-based Nanofibers via Electrospinning Technique. *Biointerface Res. Appl. Chem.* **2021**, *11*, 10801–10811. [[CrossRef](#)]
5. Cosio, M.S.; Pellicanò, A.; Gardana, C.; Fuenmayor, C.A. Debitting of Grape Juice by Electrospun Nylon Nanofibrous Membranes: Impact of Filtration on Physicochemical, Functional, and Sensory Properties. *Polymers* **2023**, *15*, 192. [[CrossRef](#)] [[PubMed](#)]
6. Agarwal, S.; Wendorff, J.H.; Greiner, A. Use of electrospinning technique for biomedical applications. *Polymer* **2008**, *49*, 5603–5621. [[CrossRef](#)]
7. Bhardwaj, N.; Kundu, S.C. Electrospinning: A fascinating fiber fabrication technique. *Biotechnol. Adv.* **2010**, *28*, 325–347. [[CrossRef](#)]

8. Luzio, A.; Canesi, E.V.; Bertarelli, C.; Caironi, M. Electrospun polymer fibers for electronic applications. *Materials* **2014**, *7*, 906–947. [[CrossRef](#)]
9. Miao, J.; Miyauchi, M.; Simmons, T.J.; Dordick, J.S.; Linhardt, R.J. Electrospinning of nanomaterials and applications in electronic components and devices. *J. Nanosci. Nanotechnol.* **2010**, *10*, 5507–5519. [[CrossRef](#)] [[PubMed](#)]
10. Lu, X.; Wang, C.; Wei, Y. One-dimensional composite nanomaterials: Synthesis by electrospinning and their applications. *Small* **2009**, *5*, 2349–2370. [[CrossRef](#)] [[PubMed](#)]
11. Fathi, S.; Saber, R.; Adabi, M.; Rasouli, R.; Douraghi, M.; Morshedi, M.; Farid-Majidi, R. Novel Competitive Voltametric Aptasensor Based on Electrospun Carbon Nanofibers-Gold Nanoparticles Modified Graphite Electrode for Salmonella enterica serovar Detection. *Biointerface Res. Appl. Chem.* **2021**, *11*, 8702–8715. [[CrossRef](#)]
12. Wang, M.; Zhao, Q. Electrospinning and electrospray for biomedical applications. In *Reference Module in Biomedical Sciences: Encyclopedia of Biomedical Engineering*; Elsevier: Amsterdam, The Netherlands, 2019.
13. Yan, G.; Niu, H.; Lin, T. Needle-less electrospinning. In *Electrospinning: Nanofabrication and Applications*; Elsevier: Amsterdam, The Netherlands, 2019; pp. 219–247.
14. Park, J.-S. Electrospinning and its applications. *Adv. Nat. Sci. Nanosci. Nanotechnol.* **2010**, *1*, 043002. [[CrossRef](#)]
15. Chen, S.; Li, R.; Li, X.; Xie, J. Electrospinning: An enabling nanotechnology platform for drug delivery and regenerative medicine. *Adv. Drug Deliv. Rev.* **2018**, *132*, 188–213. [[CrossRef](#)] [[PubMed](#)]
16. Xu, J.; Liu, X.; Zhang, Z.; Wang, L.; Tan, R.; Zhang, D. Controllable generation of nanofibers through a magnetic-field-assisted electrospinning design. *Mater. Lett.* **2019**, *247*, 19–24. [[CrossRef](#)]
17. Ghanbariasad, A.; Amoozegar, F.; Rahmani, M.; Zarenezhad, E.; Osanloo, M. Impregnated Nanofibrous Mat with Nanogel of Citrus sinensis Essential Oil as a New Type of Dressing in Cutaneous Leishmaniasis. *Biointerface Res. Appl. Chem.* **2021**, *11*, 11066–11076. [[CrossRef](#)]
18. Rahmati, M.; Mills, D.K.; Urbanska, A.M.; Saeb, M.R.; Venugopal, J.R.; Ramakrishna, S.; Mozafari, M. Electrospinning for tissue engineering applications. *Prog. Mater. Sci.* **2021**, *117*, 100721. [[CrossRef](#)]
19. Cui, W.; Zhou, Y.; Chang, J. Electrospun nanofibrous materials for tissue engineering and drug delivery. *Sci. Technol. Adv. Mater.* **2010**, *11*, 014108. [[CrossRef](#)]
20. Chen, Y.; Dong, X.; Shafiq, M.; Myles, G.; Radacsi, N.; Mo, X. Recent advancements on three-dimensional electrospun nanofiber scaffolds for tissue engineering. *Adv. Fiber Mater.* **2022**, *4*, 959–986. [[CrossRef](#)]
21. Oprea, A.E.; Ficaï, A.; Andronescu, E. Electrospun nanofibers for tissue engineering applications. In *Materials for Biomedical Engineering*; Elsevier: Amsterdam, The Netherlands, 2019; pp. 77–95.
22. Kamaci, U.D.; Peksel, A. Poly(vinyl alcohol)-based Electrospun Nanofibers: Characterization and Phytase Immobilization. *Biointerface Res. Appl. Chem.* **2022**, *12*, 7573–7583. [[CrossRef](#)]
23. Chen, K.; Hu, H.; Zeng, Y.; Pan, H.; Wang, S.; Zhang, Y.; Shi, L.; Tan, G.; Pan, W.; Liu, H. Recent advances in electrospun nanofibers for wound dressing. *Eur. Polym. J.* **2022**, 111490. [[CrossRef](#)]
24. Ghomi, E.R.; Khosravi, F.; Neisiany, R.E.; Shakiba, M.; Zare, M.; Lakshminarayanan, R.; Chellappan, V.; Abdouss, M.; Ramakrishna, S. Advances in electrospinning of aligned nanofiber scaffolds used for wound dressings. *Curr. Opin. Biomed. Eng.* **2022**, *22*, 100393.
25. Miguel, S.P.; Figueira, D.R.; Simões, D.; Ribeiro, M.P.; Coutinho, P.; Ferreira, P.; Correia, I.J. Electrospun polymeric nanofibres as wound dressings: A review. *Colloids Surf. B Biointerfaces* **2018**, *169*, 60–71. [[CrossRef](#)] [[PubMed](#)]
26. Ketabchi, N.; Dinarvand, R.; Adabi, M.; Gholami, M.; Firoozi, S.; Amanzadi, B.; Faridi-Majidi, R. Study of Third-Degree Burn Wounds Debridement and Treatment by Actinidin Enzyme Immobilized on Electrospun Chitosan/PEO Nanofibers in Rats. *Biointerface Res. Appl. Chem.* **2021**, *11*, 10358–10370. [[CrossRef](#)]
27. Manuel, C.B.J.; Jesús, V.G.L.; Aracely, S.M. Electrospinning for drug delivery systems: Drug incorporation techniques. In *Electrospinning-Material, Techniques, and Biomedical Applications*; INTECH: Rang-Du-Fliers, France, 2016; p. 14.
28. Yu, D.-G.; Zhu, L.-M.; White, K.; Branford-White, C. Electrospun nanofiber-based drug delivery systems. *Health* **2009**, *1*, 67. [[CrossRef](#)]
29. Ghosal, K.; Augustine, R.; Zaszczynska, A.; Barman, M.; Jain, A.; Hasan, A.; Kalarikkal, N.; Sajkiewicz, P.; Thomas, S. Novel drug delivery systems based on triaxial electrospinning based nanofibers. *React. Funct. Polym.* **2021**, *163*, 104895. [[CrossRef](#)]
30. Cleeton, C.; Keirouz, A.; Chen, X.; Radacsi, N. Electrospun nanofibers for drug delivery and biosensing. *ACS Biomater. Sci. Eng.* **2019**, *5*, 4183–4205. [[CrossRef](#)]
31. Tiplea, R.E.; Lemnaru, G.M.; Trusca, R.D.; Holban, A.; Kaya, M.G.A.; Dragu, L.D.; Ficaï, D.; Ficaï, A.; Bleotu, C. Antimicrobial Films based on Chitosan, Collagen, and ZnO for Skin Tissue Regeneration. *Biointerface Res. Appl. Chem.* **2021**, *11*, 11985–11995. [[CrossRef](#)]
32. Ji, G.; Chen, Z.; Li, H.; Awuye, D.E.; Guan, M.; Zhu, Y. Electrospinning-Based Biosensors for Health Monitoring. *Biosensors* **2022**, *12*, 876. [[CrossRef](#)]
33. Halicka, K.; Cabaj, J. Electrospun nanofibers for sensing and biosensing applications—A review. *Int. J. Mol. Sci.* **2021**, *22*, 6357. [[CrossRef](#)]
34. Dziemidowicz, K.; Sang, Q.; Wu, J.; Zhang, Z.; Zhou, F.; Lagaron, J.M.; Mo, X.; Parker, G.J.; Yu, D.-G.; Zhu, L.-M. Electrospinning for healthcare: Recent advancements. *J. Mater. Chem. B* **2021**, *9*, 939–951. [[CrossRef](#)]
35. Reddy, V.S.; Tian, Y.; Zhang, C.; Ye, Z.; Roy, K.; Chinnappan, A.; Ramakrishna, S.; Liu, W.; Ghosh, R. A review on electrospun nanofibers based advanced applications: From health care to energy devices. *Polymers* **2021**, *13*, 3746. [[CrossRef](#)] [[PubMed](#)]

36. Agarwal, A.; Rao, G.K.; Majumder, S.; Shandilya, M.; Rawat, V.; Purwar, R.; Verma, M.; Srivastava, C.M. Natural protein-based electrospun nanofibers for advanced healthcare applications: Progress and challenges. *3 Biotech* **2022**, *12*, 92. [[CrossRef](#)] [[PubMed](#)]
37. Vickers, N.J. Animal communication: When i'm calling you, will you answer too? *Curr. Biol.* **2017**, *27*, R713–R715. [[CrossRef](#)] [[PubMed](#)]
38. Li, Z.; Wang, C.; Li, Z.; Wang, C. Effects of working parameters on electrospinning. In *One-Dimensional Nanostructures: Electrospinning Technique and Unique Nanofibers*; Springer: Berlin/Heidelberg, Germany, 2013; pp. 15–28.
39. Huang, Z.-M.; Zhang, Y.-Z.; Kotaki, M.; Ramakrishna, S. A review on polymer nanofibers by electrospinning and their applications in nanocomposites. *Compos. Sci. Technol.* **2003**, *63*, 2223–2253. [[CrossRef](#)]
40. Hassan, C.M.; Peppas, N.A. Structure and morphology of freeze/thawed PVA hydrogels. *Macromolecules* **2000**, *33*, 2472–2479. [[CrossRef](#)]
41. Jiang, S.; Liu, S.; Feng, W. PVA hydrogel properties for biomedical application. *J. Mech. Behav. Biomed. Mater.* **2011**, *4*, 1228–1233. [[CrossRef](#)] [[PubMed](#)]
42. Kumar, A.; Han, S.S. PVA-based hydrogels for tissue engineering: A review. *Int. J. Polym. Mater. Polym. Biomater.* **2017**, *66*, 159–182. [[CrossRef](#)]
43. Kariminejad, M.; Zibaei, R.; Kolahdouz-Nasiri, A.; Mohammadi, R.; Mortazavian, A.M.; Sohrabvandi, S.; Khanniri, E.; Khorshidian, N. Chitosan/Polyvinyl Alcohol/SiO₂ Nanocomposite Films: Physicochemical and Structural Characterization. *Biointerface Res. Appl. Chem.* **2022**, *12*, 3725–3734. [[CrossRef](#)]
44. Ho, T.-C.; Chang, C.-C.; Chan, H.-P.; Chung, T.-W.; Shu, C.-W.; Chuang, K.-P.; Duh, T.-H.; Yang, M.-H.; Tyan, Y.-C. Hydrogels: Properties and applications in biomedicine. *Molecules* **2022**, *27*, 2902. [[CrossRef](#)] [[PubMed](#)]
45. Hong, Y.; Lin, Z.; Yang, Y.; Jiang, T.; Shang, J.; Luo, Z. Biocompatible Conductive Hydrogels: Applications in the Field of Biomedicine. *Int. J. Mol. Sci.* **2022**, *23*, 4578. [[CrossRef](#)]
46. Haghju, S.; Bari, M.R.; Khaled-Abad, M.A. Affecting parameters on fabrication of β -D-galactosidase immobilized chitosan/poly (vinyl alcohol) electrospun nanofibers. *Carbohydr. Polym.* **2018**, *200*, 137–143. [[CrossRef](#)]
47. Elmorsy, E.E.; Abdelghany, A.M.; Ayad, D.M.; Gammal, O.A.E. Synthesis and Physicochemical Studies of Polyvinyl Alcohol Polymer Modified with Copper Thiosemicarbazide Complex. *Lett. Appl. NanoBioSci.* **2021**, *10*, 2624–2636. [[CrossRef](#)]
48. Prabakaran, V.; Chua, K.J.; Prabakaran, V.; Chua, K.J. Latest Developments in the Desiccant-Coated Dehumidifiers. In *Advances in Desiccant Dehumidification: From Fundamentals to Applications*; Springer: Cham, Switzerland, 2021; pp. 49–88.
49. Eyssa, H.; Osman, M.; Kandil, S.; Abdelrahman, M. Effect of ion and electron beam irradiation on surface morphology and optical properties of PVA. *Nucl. Sci. Tech.* **2015**, *26*, 74–79.
50. Paipitak, K.; Pornpra, T.; Mongkontalang, P.; Techitdheer, W.; Pecharapa, W. Characterization of PVA-chitosan nanofibers prepared by electrospinning. *Procedia Eng.* **2011**, *8*, 101–105. [[CrossRef](#)]
51. Habibi, S.; Mohammadi, T.; Hmtshirazi, R.; Atyabi, F.; Kiani, M.; Asadi, A.A. A bilayer mupirocin/bupivacaine-loaded wound dressing based on chitosan/poly (vinyl alcohol) nanofibrous mat: Preparation, characterization, and controlled drug release. *Int. J. Biol. Macromol.* **2023**, *240*, 124399. [[CrossRef](#)] [[PubMed](#)]
52. Dash, M.; Chiellini, F.; Ottenbrite, R.M.; Chiellini, E. Chitosan—A versatile semi-synthetic polymer in biomedical applications. *Prog. Polym. Sci.* **2011**, *36*, 981–1014. [[CrossRef](#)]
53. Kravanja, G.; Primožič, M.; Knez, Ž.; Leitgeb, M. Chitosan-based (Nano) materials for novel biomedical applications. *Molecules* **2019**, *24*, 1960. [[CrossRef](#)]
54. Jayakumar, R.; Menon, D.; Manzoor, K.; Nair, S.V.; Tamura, H. Biomedical applications of chitin and chitosan based nanomaterials—A short review. *Carbohydr. Polym.* **2010**, *82*, 227–232. [[CrossRef](#)]
55. Gewili, N.; Abdelghany, A.M.; Mekhaimer, M.; Oraby, A. Synthesis and Optical Properties of Chitosan/polypyrrole Composite for Biological Applications. *Lett. Appl. NanoBioSci.* **2021**, *10*, 2742–2749. [[CrossRef](#)]
56. Thillaipandian, H.; Vankateshwarapuram, R. Comprehensive review on electrospinning of starch for biomedical applications. *Int. J. Biol. Macromol.* **2017**, *106*, 712–718.
57. Cheah, W.Y.; Show, P.-L.; Ng, I.-S.; Lin, G.-Y.; Chiu, C.-Y.; Chang, Y.-K. Antibacterial activity of quaternized chitosan modified nanofiber membrane. *Int. J. Biol. Macromol.* **2019**, *126*, 569–577. [[CrossRef](#)] [[PubMed](#)]
58. Szymańska, E.; Winnicka, K. Stability of chitosan—A challenge for pharmaceutical and biomedical applications. *Mar. Drugs* **2015**, *13*, 1819–1846. [[CrossRef](#)]
59. Kalantari, K.; Afifi, A.M.; Jahangirian, H.; Webster, T.J. Biomedical applications of chitosan electrospun nanofibers as a green polymer—Review. *Carbohydr. Polym.* **2019**, *207*, 588–600. [[CrossRef](#)] [[PubMed](#)]
60. Homayoni, H.; Ravandi, S.A.H.; Valizadeh, M. Electrospinning of chitosan nanofibers: Processing optimization. *Carbohydr. Polym.* **2009**, *77*, 656–661. [[CrossRef](#)]
61. Prakash, P.; Gnanaprakasam, P.; Emmanuel, R.; Arokiyaraj, S.; Saravanan, M. Green synthesis of silver nanoparticles from leaf extract of *Mimusops elengi*, Linn. for enhanced antibacterial activity against multi drug resistant clinical isolates. *Colloids Surf. B Biointerfaces* **2013**, *108*, 255–259. [[CrossRef](#)]
62. Francolini, I.; Norris, P.; Piozzi, A.; Donelli, G.; Stoodley, P. Usnic acid, a natural antimicrobial agent able to inhibit bacterial biofilm formation on polymer surfaces. *Antimicrob. Agents Chemother.* **2004**, *48*, 4360–4365. [[CrossRef](#)]

63. Pagano, C.; Ceccarini, M.R.; Calarco, P.; Scuota, S.; Conte, C.; Primavilla, S.; Ricci, M.; Perioli, L. Bioadhesive polymeric films based on usnic acid for burn wound treatment: Antibacterial and cytotoxicity studies. *Colloids Surf. B Biointerfaces* **2019**, *178*, 488–499. [[CrossRef](#)] [[PubMed](#)]
64. Paździora, W.; Podolak, I.; Grudzińska, M.; Paško, P.; Grabowska, K.; Galanty, A. Critical Assessment of the Anti-Inflammatory Potential of Usnic Acid and Its Derivatives—A Review. *Life* **2023**, *13*, 1046. [[CrossRef](#)] [[PubMed](#)]
65. Luzina, O.A.; Salakhutdinov, N.F. Usnic acid and its derivatives for pharmaceutical use: A patent review (2000–2017). *Expert Opin. Ther. Pat.* **2018**, *28*, 477–491. [[CrossRef](#)]
66. Elo, H.; Matikainen, J.; Pelttari, E. Potent activity of the lichen antibiotic (+)-usnic acid against clinical isolates of vancomycin-resistant enterococci and methicillin-resistant *Staphylococcus aureus*. *Naturwissenschaften* **2007**, *94*, 465–468. [[CrossRef](#)]
67. Gupta, V.; Verma, S.; Gupta, S.; Singh, A.; Pal, A.; Srivastava, S.; Srivastava, P.; Singh, S.; Darokar, M. Membrane-damaging potential of natural L-(–)-usnic acid in *Staphylococcus aureus*. *Eur. J. Clin. Microbiol. Infect. Dis.* **2012**, *31*, 3375–3383. [[CrossRef](#)]
68. Priya, A.; Kumar, C.B.M.; Valliammai, A.; Selvaraj, A.; Pandian, S.K. Usnic acid deteriorates acidogenicity, acidurance and glucose metabolism of *Streptococcus mutans* through downregulation of two-component signal transduction systems. *Sci. Rep.* **2021**, *11*, 1374. [[CrossRef](#)]
69. Ingolfssdottir, K. Usnic acid. *Phytochemistry* **2002**, *61*, 729–736. [[CrossRef](#)]
70. Cocchietto, M.; Skert, N.; Nimis, P.; Sava, G. A review on usnic acid, an interesting natural compound. *Naturwissenschaften* **2002**, *89*, 137–146. [[CrossRef](#)] [[PubMed](#)]
71. Chandika, P.; Khan, F.; Heo, S.-Y.; Kim, Y.-M.; Yi, M.; Jung, W.-K. Enhanced wound-healing capability with inherent antimicrobial activities of usnic acid incorporated poly (ϵ -caprolactone)/decellularized extracellular matrix nanofibrous scaffold. *Biomater. Adv.* **2022**, *140*, 213046. [[CrossRef](#)] [[PubMed](#)]
72. Francolini, I.; Taresco, V.; Crisante, F.; Martinelli, A.; D’Ilario, L.; Piozzi, A. Water soluble usnic acid-polyacrylamide complexes with enhanced antimicrobial activity against *Staphylococcus epidermidis*. *Int. J. Mol. Sci.* **2013**, *14*, 7356–7369. [[CrossRef](#)] [[PubMed](#)]
73. Nithyanand, P.; Beema Shafreen, R.M.; Muthamil, S.; Karutha Pandian, S. Usnic acid, a lichen secondary metabolite inhibits Group A *Streptococcus* biofilms. *Antonie Van Leeuwenhoek* **2015**, *107*, 263–272. [[CrossRef](#)]
74. Ivanova, V.; Graefe, U.; Schlegel, B.; Kolarova, M.; Aleksieva, K.; Najdenski, H.; Tzvetkova, I.; Chipeva, V. Usnic Acid, Metabolite from *Neuropogon* Sp., An Antarctic Lichen Isolation, Structure Elucidation and Biological Activity. *Biotechnol. Biotechnol. Equip.* **2004**, *18*, 66–71. [[CrossRef](#)]
75. Paduraru, A.V.; Oprea, O.; Musuc, A.M.; Vasile, B.S.; Iordache, F.; Andronescu, E. Influence of Terbium Ions and Their Concentration on the Photoluminescence Properties of Hydroxyapatite for Biomedical Applications. *Nanomaterials* **2021**, *11*, 2442. [[CrossRef](#)] [[PubMed](#)]
76. Shi, S.; Si, Y.; Han, Y.; Wu, T.; Iqbal, M.I.; Fei, B.; Li, R.K.; Hu, J.; Qu, J. Recent progress in protective membranes fabricated via electrospinning: Advanced materials, biomimetic structures, and functional applications. *Adv. Mater.* **2022**, *34*, 2107938. [[CrossRef](#)] [[PubMed](#)]
77. Xie, X.; Chen, Y.; Wang, X.; Xu, X.; Shen, Y.; Khan, A.u.R.; Aldalbahi, A.; Fetz, A.E.; Bowlin, G.L.; El-Newehy, M.; et al. Electrospinning nanofiber scaffolds for soft and hard tissue regeneration. *J. Mater. Sci. Technol.* **2020**, *59*, 243–261. [[CrossRef](#)]
78. Mohammadalizadeh, Z.; Bahremandi-Toloue, E.; Karbasi, S. Recent advances in modification strategies of pre- and post-electrospinning of nanofiber scaffolds in tissue engineering. *React. Funct. Polym.* **2022**, *172*, 105202. [[CrossRef](#)]
79. Usawattanakul, N.; Torgbo, S.; Sukyai, P.; Khantayanuwong, S.; Puangsins, B.; Srichola, P. Development of Nanocomposite Film Comprising of Polyvinyl Alcohol (PVA) Incorporated with Bacterial Cellulose Nanocrystals and Magnetite Nanoparticles. *Polymers* **2021**, *13*, 1778. [[CrossRef](#)] [[PubMed](#)]
80. Modrogan, C.; Căprărescu, S.; Dăncilă, A.M.; Orbuleț, O.D.; Grumezescu, A.M.; Purcar, V.; Radițoiu, V.; Fierascu, R.C. Modified Composite Based on Magnetite and Polyvinyl Alcohol: Synthesis, Characterization, and Degradation Studies of the Methyl Orange Dye from Synthetic Wastewater. *Polymers* **2021**, *13*, 3911. [[CrossRef](#)]
81. Cazón, P.; Velázquez, G.; Vázquez, M. Characterization of bacterial cellulose films combined with chitosan and polyvinyl alcohol: Evaluation of mechanical and barrier properties. *Carbohydr. Polym.* **2019**, *216*, 72–85. [[CrossRef](#)] [[PubMed](#)]
82. Fernandes Queiroz, M.; Melo, K.R.T.; Sabry, D.A.; Sasaki, G.L.; Rocha, H.A.O. Does the Use of Chitosan Contribute to Oxalate Kidney Stone Formation? *Mar. Drugs* **2015**, *13*, 141–158. [[CrossRef](#)]
83. Huang, C.-C. Design and Characterization of a Bioinspired Polyvinyl Alcohol Matrix with Structural Foam-Wall Microarchitectures for Potential Tissue Engineering Applications. *Polymers* **2022**, *14*, 1585. [[CrossRef](#)] [[PubMed](#)]
84. Sadiq, N.M.; Aziz, S.B.; Kadir, M.F.Z. Development of Flexible Plasticized Ion Conducting Polymer Blend Electrolytes Based on Polyvinyl Alcohol (PVA): Chitosan (CS) with High Ion Transport Parameters Close to Gel Based Electrolytes. *Gels* **2022**, *8*, 153. [[CrossRef](#)] [[PubMed](#)]
85. Al-Tayyar, N.A.; Youssef, A.M.; Al-Hindi, R.R. Antimicrobial packaging efficiency of ZnO-SiO₂ nanocomposites infused into PVA/CS film for enhancing the shelf life of food products. *Food Packag. Shelf Life* **2020**, *25*, 100523. [[CrossRef](#)]
86. Kokubo, T.; Kushitani, H.; Sakka, S.; Kitsugi, T.; Yamamuro, T. Solutions able to reproduce in vivo surface-structure changes in bioactive glass-ceramic A-W3. *J. Biomed. Mater. Res.* **1990**, *24*, 721–734. [[CrossRef](#)] [[PubMed](#)]

87. Iordache, F.; Grumezescu, V.; Grumezescu, A.M.; Curuțiu, C.; Dițu, L.M.; Socol, G.; Ficai, A.; Trușcă, R.; Holban, A.M. Gamma-cyclodextrin/usnic acid thin film fabricated by MAPLE for improving the resistance of medical surfaces to *Staphylococcus aureus* colonization. *Appl. Surf. Sci.* **2015**, *336*, 407–412. [[CrossRef](#)]
88. Vijayakumar, C.S.; Viswanathan, S.; Kannappa Reddy, M.; Parvathavarthini, S.; Kundu, A.B.; Sukumar, E. Anti-inflammatory activity of (+)-usnic acid. *Fitoterapia* **2000**, *71*, 564–566. [[CrossRef](#)]
89. Mayer, M.; O'Neill, M.A.; Murray, K.E.; Santos-Magalhães, N.S.; Carneiro-Leão, A.M.A.; Thompson, A.M.; Appleyard, V.C.L. Usnic acid: A non-genotoxic compound with anti-cancer properties. *Anti-Cancer Drugs* **2005**, *16*, 805–809. [[CrossRef](#)] [[PubMed](#)]
90. Grumezescu, V.; Socol, G.; Grumezescu, A.M.; Holban, A.M.; Ficai, A.; Trușcă, R.; Bleotu, C.; Balaure, P.C.; Cristescu, R.; Chifiriuc, M.C. Functionalized antibiofilm thin coatings based on PLA–PVA microspheres loaded with usnic acid natural compounds fabricated by MAPLE. *Appl. Surf. Sci.* **2014**, *302*, 262–267. [[CrossRef](#)]
91. Grumezescu, A.M.; Saviuc, C.; Chifiriuc, M.C.; Hristu, R.; Mihaiescu, D.E.; Balaure, P.; Stanciu, G.; Lazar, V. Inhibitory Activity of Fe₃O₄/Oleic Acid/Usnic Acid—Core/Shell/Extra-Shell Nanofluid on *S. aureus* Biofilm Development. *IEEE Trans. NanoBioSci.* **2011**, *10*, 269–274. [[CrossRef](#)] [[PubMed](#)]
92. Grumezescu, A.M.; Cotar, A.I.; Andronescu, E.; Ficai, A.; Ghitulica, C.D.; Grumezescu, V.; Vasile, B.S.; Chifiriuc, M.C. In vitro activity of the new water-dispersible Fe₃O₄@usnic acid nanostructure against planktonic and sessile bacterial cells. *J. Nanopart. Res.* **2013**, *15*, 1766. [[CrossRef](#)]
93. Holban, A.M.; Grumezescu, A.M.; Andronescu, E.; Grumezescu, V.; Chifiriuc, C.M.; Radulescu, R. Material nanostructurat bioactiv magnetita-acid usnic cu activitate antimicrobiana/magnetite-usnic acid nanostructured bioactive material with antimicrobial activity. *Rev. Romana Mater.* **2013**, *43*, 402.
94. Guzun, A.S.; Stroescu, M.; Jinga, S.I.; Voicu, G.; Grumezescu, A.M.; Holban, A.M. Plackett–Burman experimental design for bacterial cellulose-silica composites synthesis. *Mater. Sci. Eng. C* **2014**, *42*, 280–288. [[CrossRef](#)]
95. Hinderer, S.; Layland, S.L.; Schenke-Layland, K. ECM and ECM-like materials—Biomaterials for applications in regenerative medicine and cancer therapy. *Adv. Drug Deliv. Rev.* **2016**, *97*, 260–269. [[CrossRef](#)]
96. Ladd, M.R.; Hill, T.K.; Yoo, J.J.; Lee, S.J. Electrospun nanofibers in tissue engineering. In *Nanofibers-Production, Properties and Functional Applications*; InTechOpen: London, UK, 2011; pp. 347–373.
97. Sun, D.; Chang, C.; Li, S.; Lin, L. Near-field electrospinning. *Nano Lett.* **2006**, *6*, 839–842. [[CrossRef](#)] [[PubMed](#)]
98. Zhou, F.; Cui, C.; Sun, S.; Wu, S.; Chen, S.; Ma, J.; Li, C.M. Electrospun ZnO-loaded chitosan/PCL bilayer membranes with spatially designed structure for accelerated wound healing. *Carbohydr. Polym.* **2022**, *282*, 119131. [[CrossRef](#)]
99. Vargas-Osorio, Z.; Ruther, F.; Chen, S.; Sengupta, S.; Liverani, L.; Michálek, M.; Galusek, D.; Boccaccini, A.R. Environmentally friendly fabrication of electrospun nanofibers made of polycaprolactone, chitosan and κ -carrageenan (PCL/CS/ κ -C). *Biomed. Mater.* **2022**, *17*, 045019. [[CrossRef](#)]
100. Ali, E.A.; Abo-Salem, H.M.; Arafa, A.A.; Nada, A.A. Chitosan Schiff base electrospun fabrication and molecular docking assessment for nonleaching antibacterial nanocomposite production. *Cellulose* **2023**, *30*, 3505–3522. [[CrossRef](#)] [[PubMed](#)]
101. Pilavci, E.; Ayran, M.; Ulubay, D.; Kaya, E.; Tinaz, G.; Bingol Ozakpinar, O.; Sancakli, A.; Gunduz, O. Fabrication and characterization of electrospun GelMA/PCL/CS nanofiber composites for wound dressing applications. *J. Bioact. Compat. Polym.* **2023**, *38*, 08839115221138777. [[CrossRef](#)]
102. Doostan, M.; Doostan, M.; Mohammadi, P.; Khoshnevisan, K.; Maleki, H. Wound healing promotion by flaxseed extract-loaded polyvinyl alcohol/chitosan nanofibrous scaffolds. *Int. J. Biol. Macromol.* **2023**, *228*, 506–516. [[CrossRef](#)]
103. Chopra, H.; Bibi, S.; Kumar, S.; Khan, M.S.; Kumar, P.; Singh, I. Preparation and evaluation of chitosan/PVA based hydrogel films loaded with honey for wound healing application. *Gels* **2022**, *8*, 111. [[CrossRef](#)]
104. Adeli, H.; Khorasani, M.T.; Parvazinia, M. Wound dressing based on electrospun PVA/chitosan/starch nanofibrous mats: Fabrication, antibacterial and cytocompatibility evaluation and in vitro healing assay. *Int. J. Biol. Macromol.* **2019**, *122*, 238–254. [[CrossRef](#)]
105. Kumar, S.; Ye, F.; Dobretsov, S.; Dutta, J. Chitosan nanocomposite coatings for food, paints, and water treatment applications. *Appl. Sci.* **2019**, *9*, 2409. [[CrossRef](#)]
106. De Britto, D.; Campana-Filho, S.P. Kinetics of the thermal degradation of chitosan. *Thermochim. Acta* **2007**, *465*, 73–82. [[CrossRef](#)]
107. Dehghani, N.; Haghirsadat, F.; Yazdian, F.; Sadeghian-Nodoushan, F.; Ghasemi, N.; Mazaheri, F.; Pourmadadi, M.; Naghib, S.M. Chitosan/silk fibroin/nitrogen-doped carbon quantum dot/ α -tricalcium phosphate nanocomposite electrospun as a scaffold for wound healing application: In vitro and in vivo studies. *Int. J. Biol. Macromol.* **2023**, *238*, 124078. [[CrossRef](#)]
108. Kamaci, M.; Kaya, I. Chitosan based hybrid hydrogels for drug delivery: Preparation, biodegradation, thermal, and mechanical properties. *Polym. Adv. Technol.* **2023**, *34*, 779–788. [[CrossRef](#)]
109. Saudi, S.; Jun, S.; Fialkova, S.; Surendran, V.; Chandrasekaran, A.; Bhattarai, S.R.; Sankar, J.; Bhattarai, N. Incorporating nanoconfined chitin-fibrils in poly (ϵ -caprolactone) membrane scaffolds improves mechanical and chemical properties for biomedical application. *J. Biomed. Mater. Res. Part A* **2023**, *111*, 1185–1199. [[CrossRef](#)] [[PubMed](#)]
110. Snetkov, P.; Morozkina, S.; Olekhnovich, R.; Vu, T.H.N.; Tyanutova, M.; Uspenskaya, M. Curcumin/usnic acid-loaded electrospun nanofibers based on hyaluronic acid. *Materials* **2020**, *13*, 3476. [[CrossRef](#)]
111. Najafi, R.; Chahsetareh, H.; Pezeshki-Modaress, M.; Aleemardani, M.; Simorgh, S.; Davachi, S.M.; Alizadeh, R.; Asghari, A.; Hassanzadeh, S.; Bagher, Z. Alginate sulfate/ECM composite hydrogel containing electrospun nanofiber with encapsulated human adipose-derived stem cells for cartilage tissue engineering. *Int. J. Biol. Macromol.* **2023**, *238*, 124098. [[CrossRef](#)]

112. Wang, M.; Deng, Z.; Guo, Y.; Xu, P. Engineering functional natural polymer-based nanocomposite hydrogels for wound healing. *Nanoscale Adv.* **2023**, *5*, 27–45. [[CrossRef](#)]
113. Galla, R.; Ferrari, S.; Ruga, S.; Mantuano, B.; Rosso, G.; Tonello, S.; Rosa, L.; Valenti, P.; Uberti, F. Effects of Usnic Acid to Prevent Infections by Creating a Protective Barrier in an In Vitro Study. *Int. J. Mol. Sci.* **2023**, *24*, 3695. [[CrossRef](#)] [[PubMed](#)]
114. Wang, H.; Xuan, M.; Huang, C.; Wang, C. Advances in research on bioactivity, toxicity, metabolism, and pharmacokinetics of usnic acid in vitro and in vivo. *Molecules* **2022**, *27*, 7469. [[CrossRef](#)]
115. Ibrahim, M.A.; Alhalafi, M.H.; Emam, E.-A.M.; Ibrahim, H.; Mosaad, R.M. A Review of Chitosan and Chitosan Nanofiber: Preparation, Characterization, and Its Potential Applications. *Polymers* **2023**, *15*, 2820. [[CrossRef](#)]
116. Anjum, S.; Rahman, F.; Pandey, P.; Arya, D.K.; Alam, M.; Rajinikanth, P.S.; Ao, Q. Electrospun Biomimetic Nanofibrous Scaffolds: A Promising Prospect for Bone Tissue Engineering and Regenerative Medicine. *Int. J. Mol. Sci.* **2022**, *23*, 9206. [[CrossRef](#)]
117. Cui, J.; Yu, X.; Shen, Y.; Sun, B.; Guo, W.; Liu, M.; Chen, Y.; Wang, L.; Zhou, X.; Shafiq, M. Electrospinning Inorganic Nanomaterials to Fabricate Bionanocomposites for Soft and Hard Tissue Repair. *Nanomaterials* **2023**, *13*, 204. [[CrossRef](#)]
118. Sapkota, S.; Chou, S.F. Electrospun Chitosan-based Fibers for Wound Healing Applications. *J. Biomater.* **2020**, *4*, 51–57. [[CrossRef](#)] [[PubMed](#)]
119. Howden, B.P.; Giulieri, S.G.; Wong Fok Lung, T.; Baines, S.L.; Sharkey, L.K.; Lee, J.Y.; Hachani, A.; Monk, I.R.; Stinear, T.P. *Staphylococcus aureus* host interactions and adaptation. *Nat. Rev. Microbiol.* **2023**, *21*, 380–395. [[CrossRef](#)] [[PubMed](#)]

Disclaimer/Publisher’s Note: The statements, opinions and data contained in all publications are solely those of the individual author(s) and contributor(s) and not of MDPI and/or the editor(s). MDPI and/or the editor(s) disclaim responsibility for any injury to people or property resulting from any ideas, methods, instructions or products referred to in the content.